JOC The Journal of Organic Chemistry

Article

pubs.acs.org/joc

Phenylene-Diimine-Capped Conjugate of Lower Rim 1,3-Calix[4]Arene As Molecular Receptor for Mg^{2+} via Arm Conformational Changes Followed by Aggregation and Mimicking the Species by Molecular Mechanics

Anita Nehra, Vijaya Kumar Hinge, and Chebrolu Pulla Rao*

Department of Chemistry, Indian Institute of Technology, Powai, Mumbai - 400076, India

Supporting Information

ABSTRACT: A phenylene-diimine-capped conjugate of lower rim 1,3-calix[4]-arene (**L**) was synthesized, characterized, and shown to selectively bind to Mg^{2+} using its capped arms. This results in a selective recognition of Mg^{2+} through eliciting fluorescence enhancement of ~70 fold with a detection limit of 40 ± 5 ppb. However, in the presence of blood serum, the lowest detection limit is 209 ± 10 ppb (0.2 μM). The binding of Mg^{2+} to **L** is authenticated by absorption and ^{1}H NMR data. The Job's plot derived on the basis of the absorption data showed 1:1 stoichiometry between the receptor and Mg^{2+}. The 1:1 species was further confirmed through ESI MS, that is, being supported by the isotope peak pattern authenticating the presence of Mg^{2+} in the complex. The **L** binds Mg^{2+} octahedrally using the tetradentate L^{2-} and two additional acetic acid moieties by bringing conformational changes as studied on the basis of MM computations. The conformational changes that occur in the capped arms upon Mg^{2+} binding were supported experimentally by NOESY. AFM and SEM studies showed that spherical particles of **L** are modified into flower and chain type aggregates upon complexation with Mg^{2+}, confirming the supramolecular behavior of the species formed.

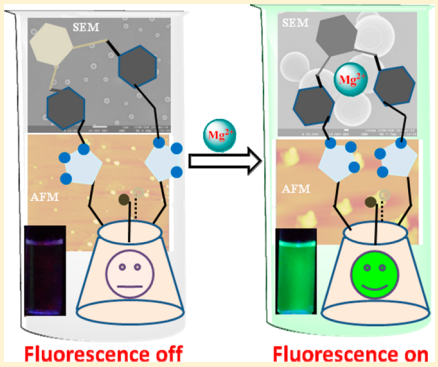

INTRODUCTION

Magnesium is one of the abundant divalent cations of biological systems and plays a critical role in cellular signaling and in pathological, neurological, and muscular functions.[1,2] Therefore, the selective detection of Mg^{2+} among the biologically abundant ions like Na^+, K^+, and Ca^{2+} has been one of the main concerns of chemical biology, while the task poses challenges to chemists in order to design and synthesize molecular systems suitable for its selective recognition. A few, small molecular fluorescence-based chemosensors for Mg^{2+} exhibited 36- and 47-fold enhancement in intensity.[3,4] Ratiometric chemosensors were developed for Mg^{2+} by dipyrenyl calixazacrown and phenanthroimidazole calix[4]arene-diamide derivatives with fluorescence enhancement of 4- and 16-fold, respectively.[5] As the sensitive detection of Mg^{2+} is essential in order to extend its application to biological conditions, the search for selective receptors, particularly the one that is based on a supramolecular system such as calixarene, continues to intrigue chemists. The receptor that is designed based on calix[4]arene would utilize additional advantages arising from its supramolecular behavior. Therefore, herein, we report the synthesis and characterization of phenylene diimine-capped lower rim 1,3-dicalix[4]arene conjugate (**L**) and show its utility as a selective receptor for Mg^{2+} even in a medium containing blood serum by demonstrating that the Mg^{2+} indeed coordinates to **L** and this introduces conformational changes in the arms of the receptor. The experimentally determined species of the 1:1 complex has been further translated into its computational model to establish the structural features of the species of recognition. The use of supramolecular features in differentiating the receptor from its magnesium complex has been demonstrated by microscopy.

RESULTS AND DISCUSSION

Design, Synthesis and Characterization of L. Our research group has been extensively involved in developing molecular receptors for transition metal ions using 1,3-diconjugates of calix[4]arene having open arms. However, if such open arms are connected together through capping, the resulting system would have certain limitations on its conformational freedom. In addition, if the receptor were to provide an N_2O_2 binding core, this would be important in selective recognition of alkali or alkaline earth ions. Thus, the phenylene diimine-capped lower rim 1,3-dicalix[4]arene conjugate, **L**, has been synthesized by going through a number of steps given in Scheme 1 (SI 01 in the Supporting Information). The final receptor and its precursors were characterized by different techniques including ^{1}H and ^{13}C NMR, and ESI MS and the cooresponding data has been given in the Experimental Section. The presence of two doublets observed at 3.3 and 4.1 ppm in ^{1}H NMR spectrum clearly

Received: April 22, 2014
Published: May 30, 2014

   dx.doi.org/10.1021/jo500892r | J. Org. Chem. 2014, 79, 5763−5770

Scheme 1. [a]

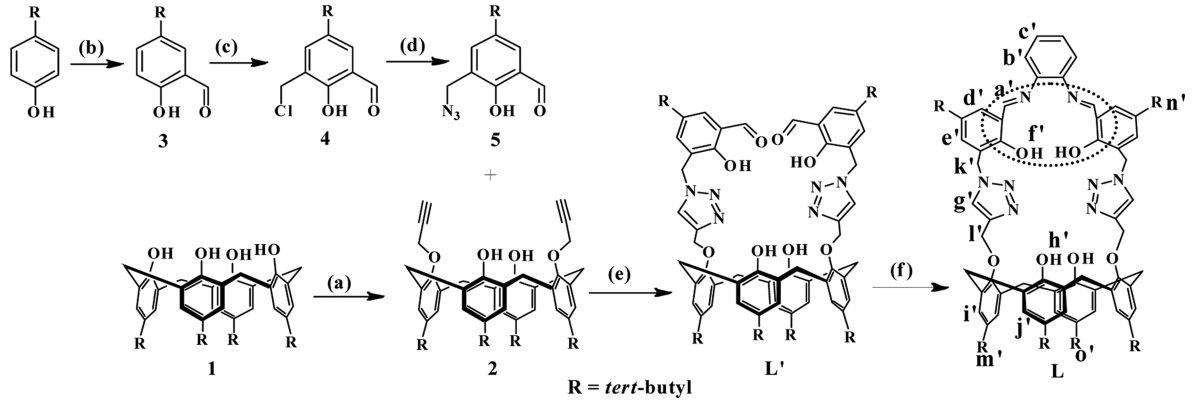

[a]Reagents and conditions: (a) K_2CO_3, propargyl bromide, acetone, reflux, 12 h, (82%); (b) $SnCl_4$, $(HCHO)_n$, Bu_3N, toluene, (55%); (c) HCl, HCHO, (85%); (d) NaN_3, DMF, (90%); (e) **5**, $CuSO_4{\cdot}5H_2O$, soduim ascorbate, dichloromethane/water (1:1), rt, 12 h, (~90%); (f) *o*-phenylenediamine, CH_3OH, rt, 12 h, (74%). The percent values shown in the brackets are yields of the products.

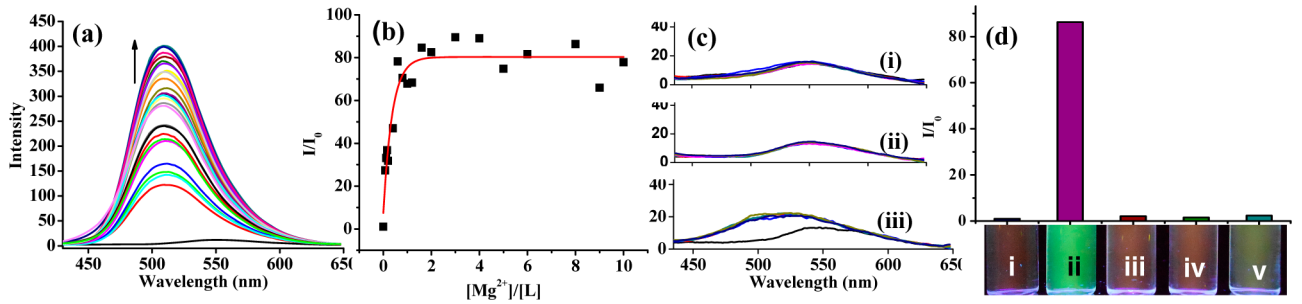

Figure 1. Fluorescence titration of **L** {25 μL of 5 μM solution} with M^{n+} {5 μM, variable volume} acetonitrile: (a) Fluorescence spectra from the titration of **L** with Mg^{2+} (λ_{ex} = 339 nm). (b) Relative intensity plot of titration of **L** with Mg^{2+}. (c) Fluorescence spectra obtained during the titration of **L** with M^{n+}: (i) Na^+, (ii) K^+ and (iii) Ca^{2+}. (d) Histogram showing the relative intensity of emission and the vials show visual color under 365 nm light. The vials are (i) = **L**, (ii) = **L**+Mg^{2+}, (iii) = **L** + Na^+, (iv) = **L** + K^+, (v) = **L** + Ca^{2+}.

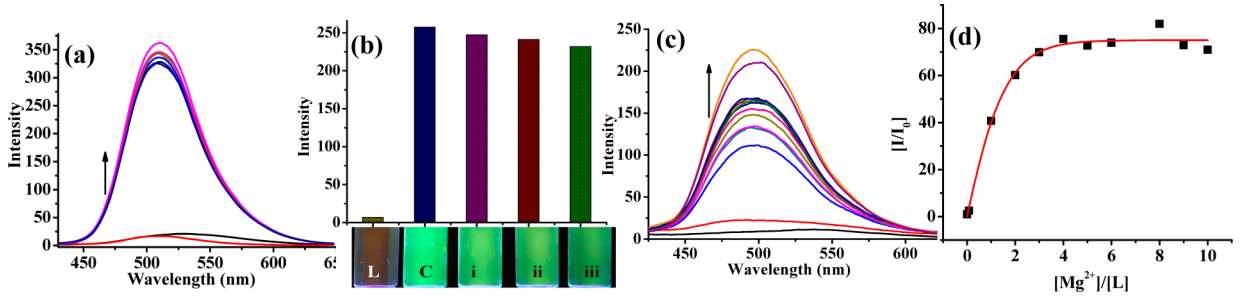

Figure 2. Competitive ion fluorescence titration: (a) Spectral traces for the titration of **L** (black) and {**L** + a mixture of (Na^+ + K^+ + Ca^{2+})} (red) followed by incremental addition of Mg^{2+} in acetonitrile (all other spectra having fluorescence enhancement). (b) Histogram showing the competitive metal ion titration response of [**L** + Mg^{2+}] with other ions and the same vials under 365 UV light. Here, (C) = {**L** + Mg^{2+}}; (i) = C + Na^+; (ii) = C + K^+; (iii) = C + Ca^{2+}; [**L**] = 5 μM; [Mg^{2+}] = 25 μM; [M^{n+}] = 50 μM. (c) Shows titration of {**L**+Na^+} with Mg^{2+} where [Na^+] = 167 mM. (d) Relative intensity plot of **L** with Mg^{2+} in the presence of blood serum taken in 10% H_2O–acetonitrile.

supports the cone conformation for **L** even after forming the cap.[6]

Selectivity toward Mg^{2+}. The **L** exhibits weak fluorescence in acetonitrile. The utility of **L** in recognizing Mg^{2+} has been investigated on the basis of its preference toward binding biologically relevant alkali and alkaline earth ions. The interaction of **L** with such ions has been studied by emission, absorption, and ^{1}H NMR spectral titrations, and the species have been supported by ESI mass spectrometry and were further modeled by molecular mechanics. The conformational changes that occur in **L** in the complex were explored by both experimental and computational methods.

Fluorescence Studies. **L** exhibits weak fluorescence emission at 553 nm when excited at 339 nm in acetonitrile due to the excited-state proton transfer (ESPT) from salicyl-OH to the imine-N, as also reported by us earlier in the case of a different molecular system.[7] Titration of **L** with Mg^{2+} results in the chelation-enhanced fluorescence intensity by ~70 fold (Figure 1a,b) that is accompanied by a blue shift of 43 nm. The enhancement in the fluorescence emission is saturated ~1 equiv of Mg^{2+} suggesting a stoichiometric reaction with **L** in its complexation. Based on this data, the binding constant derived using Benesi–Hildebrand equation is (3.3 ± 0.2) × 10^5 M^{-1} (SI 02 in the Supporting Information), and the minimum

dx.doi.org/10.1021/jo500892r | J. Org. Chem. 2014, 79, 5763–5770

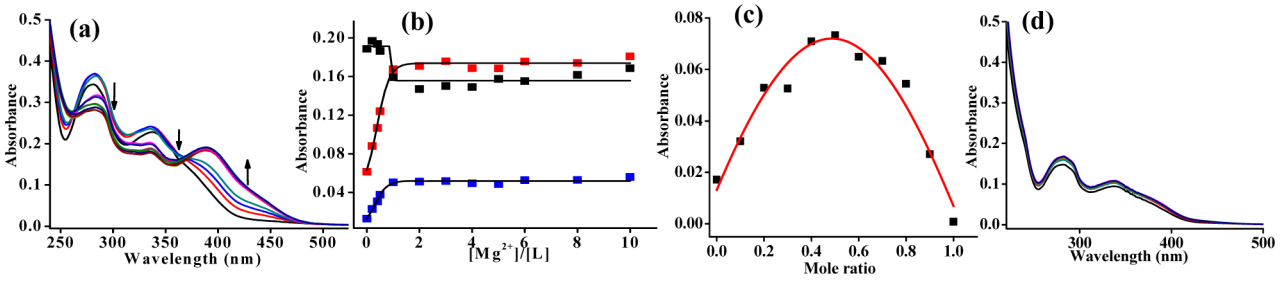

Figure 3. Absorption titration of **L** {25 μL of 5 μM solution} with M^{n+} {5 μM, variable volume} in acetonitrile. (a) Absorption spectra obtained the titration of **L** with Mg^{2+}. (b) Plots of absorbance vs mole ratio for different bands for the titration given under (a) where the blue, red and black plots correspond to 450, 400, and 355 nm bands, respectively. (c) Job's plot obtained from the absorption titration data of **L** with Mg^{2+}. (d) Absorption spectra obtained when **L** is titrated with Ca^{2+}.

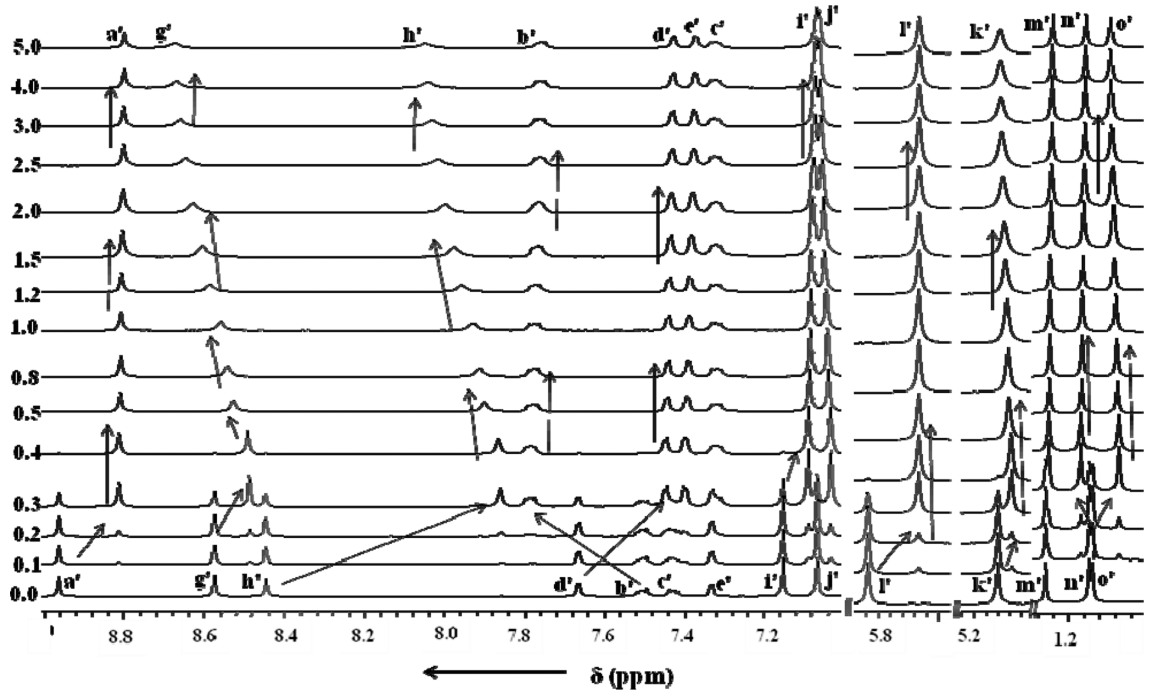

Figure 4. ^{1}H NMR spectra for the titration of **L** with different mole ratios of Mg^{2+} (numbers given on the left end of each spectrum) in DMSO-d^6. The peaks are labeled, and corresponding labeling can be read from Scheme 1

detection limit is 40 ± 5 ppb (2 μM) (SI 03 in the Supporting Information). The quantum yield of **L** raises from 0.0011 to 0.0065 upon addition of Mg^{2+}, viz., the formation of its complex, {**L**+Mg^{2+}} (SI 04 in the Supporting Information). A ratiometric chemosensor of Mg^{2+} based on calix[4]arene diamide[5b] showed the detection limit of 13.8 μM in DMSO and another small molecular benzimidazole derivative[4b] exhibited the chromogenic sensing of Mg^{2+} with a detection range of 3−100 μM. Thus, the present system reveals that the **L** reported in this paper exhibits higher fluorescence sensitivity toward Mg^{2+} than those reported in the literature.[4b,5b]

Similar titrations carried out with other biologically relevant alkali and alkaline earth ions, viz., Na^+, K^+, and Ca^{2+}, exhibited no significant enhancement in the fluorescence intensity (Figure 1c, d) (SI 05 in the Supporting Information). Under the UV light of 365 nm, the solution of **L** is nonfluorescent, while the same exhibits intense yellowish green fluorescent color in the presence of Mg^{2+}. However, Na^+, K^+, and Ca^{2+}, do not show such fluorescent color (Figure 1d). The fluorescence intensity of **L** observed with Mg^{2+} is not altered even in the presence of excess mole ratio of Na^+, K^+, or Ca^{2+}, and/or a combination of these ions, suggesting that the biologically relevant alkali and alkaline earth ions of Mg^{2+} do not compete for **L** when it is bound to Mg^{2+} (Figure 2a, b) (SI 06 in the Supporting Information).

Receptor Functioning in Blood Serum Milieu. In order to find out whether the receptor **L** can function in blood serum milieu, the fluorescent mixture of {**L** + Mg^{2+}} has been titrated by blood serum and found that the fluorescence intensity of the receptor complex persists, though the number of folds of enhancement is reduced in this medium (Figure 2d). The same result is true even when the titrations were carried out in the presence of 170 mM of Na^+, suggesting that the presence of a large concentration of Na^+ is not a deterrent for the detection of Mg^{2+} (Figure 2c). Thus, the fluorescence emission intensity shows ∼20 fold enhancement with Mg^{2+} in the medium of blood serum milieu, and the **L** is still suitable for detecting a minimum concentration of 209 ± 10 ppb (8.7 μM) (Figure 2d and SI 03 in the Supporting Information). The diluted blood plasma that is used in the present study still possesses ∼17 μM concentration of Mg^{2+}, which is certainly higher than the observed minimum detection limit of Mg^{2+} by **L** in the blood

dx.doi.org/10.1021/jo500892r | J. Org. Chem. 2014, 79, 5763−5770

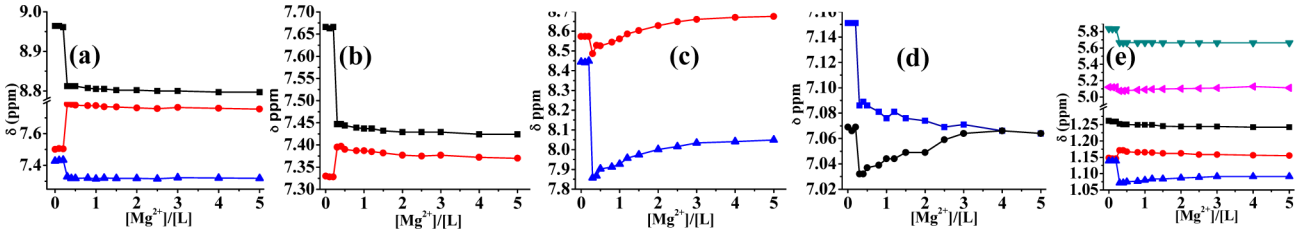

Figure 5. Chemical shift vs mole ratio plots of different protons from ^{1}H NMR spectra for the titration of **L** with different mole ratios of Mg^{2+} in DMSO-d^6. Proton labelings for different colored plots are (a) black (a′), red (b′), blue (c′); (b) black (d′), red (e′); (c) red (g′), blue (h′); (d) blue (i′), black (j′), and (e) blue (o′), red (n′), black (m′), pink (k′), green (l′).

plasma solution. All this suggests that **L** is robust enough to detect Mg^{2+} even in the biological fluids. To our knowledge, no other small-molecular receptor reported for Mg^{2+} was studied in blood serum milieu.

Absorption Studies. While the fluorescence titration studies reveal the selective sensing of Mg^{2+} to **L**, actual binding of Mg^{2+} to **L** has been confirmed by performing the absorption studies. The spectra reveal that the absorbance of the original bands of **L** observed at ∼285 and ∼355 nm decreases as a function of the added $[Mg^{2+}]$. During the titration, two new bands were observed at 400 and 450 nm and their absorbance increases as a function of added $[Mg^{2+}]$ (Figure 3a,b). Similar titrations carried out with Na^+, K^+, and Ca^{2+} did not exhibit such changes, once again confirming the nonbinding nature of these ions to **L**, and the corresponding spectra for the titration of Ca^{2+} are shown in Figure 3d (SI 07 in the Supporting Information). This is attributed to the fact that, while Mg^{2+} prefers ether-type oxygens, the Ca^{2+} prefers to bind to carboxylate moieties as noticed in the biological systems. The stoichiometry of the complex formed between **L** and Mg^{2+} is 1:1 as derived on the basis of the Job's plot (Figure 3c) and its association constant, $K_a = (1.10 \pm 0.02) \times 10^5$ M^{-1}. The K_a observed from the absorption data agrees well with that derived from the fluorescence data and the binding of Mg^{2+} to **L** is strong. Absorption titrations of **L** carried out using magnesium acetate show similar changes wherein sharp isosbestic points observed reflect on the fact that the acetate ion can act as a better base than the perchlorate ion (SI 08 in the Supporting Information).

Binding of Mg^{2+} to L by ^{1}H NMR. ^{1}H NMR titrations also supported the binding of Mg^{2+} to **L**. During the titration, the concentration of **L** was kept constant, and the $[L]/[Mg^{2+}]$ mole ratio was increased (Figure 4). Upon addition of magnesium acetate to **L**, the peak corresponding to the salicylic−OH diminishes and completely disappears within ∼1 equiv, suggesting the removal of these protons by the acetate moiety (SI 09 in the Supporting Information). In the titration of **L** with Mg^{2+}, the chemical shifts of most of the protons are shifted from marginal to considerable extents, and these changes could be categorized as upfield or downfield shifts at lower equivalents, while a reverse trend is being exhibited at higher equivalents, and all these can be noted from the spectra given in Figure 4.

While the protons "a′", "d′", "i′", "m′" and "l′" are shifted upfield, the "c′", "g′", "h′", "j′", "o′" and "k′" are shifted upfield at lower equivalents of Mg^{2+} and then move to downfield at higher concentrations of Mg^{2+}. Another set of protons, "e′" and "b′", was shifted only to the downfield. All these can be seen from the plots of chemical shifts given in Figure 5. The NMR titration data supports the fact that at lower equivalents, the salt is effective in deprotonation of the phenolic−OH, resulting in anionic **L**, which in turn results in improving the binding affinity of Mg^{2+} to **L** at higher equivalents. The arm conformational changes that occur during this process were demonstrated by 2D NMR as reported in this contribution. However, in all these titrations, the presence of two doublets observed at 3.2 and 4.1 ppm clearly supports that the cone conformation is maintained for **L** even in the complex.

Determination of the Mass of the Species of Recognition by ESI MS. All the studies suggests that the arm-N_2O_2 acts as core for Mg^{2+} binding. The ESI MS spectrum obtained for the *in situ* complex results in a molecular ion peak at m/z = 1287 that corresponds to $[L + Mg + H]^+$, and the isotopic peak pattern supports the presence of magnesium (Figure 6a, b). The 1:1 complex species was also observed

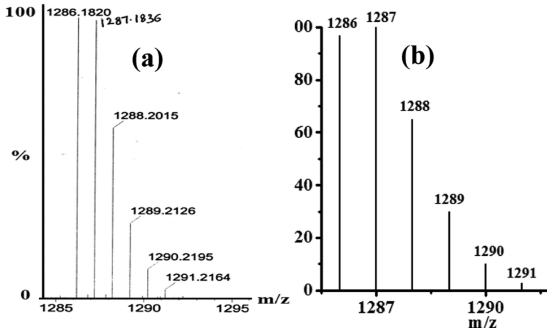

Figure 6. ESI mass spectra for the 1:1 complex of **L** with Mg^{2+} along with isotopic peak pattern: (a) observed and (b) calculated.

when **L** was titrated with magnesium acetate. In addition, peaks corresponding to one- and two-acetate-bound species were also observed in ESI MS at m/z = 1386 $[L + Mg + CH_3COOH + K]^+$ and 1445 $[L + Mg + 2CH_3COOH + K]^+$ respectively (SI 10 in the Supporting Information).

Computation Modeling of the Mg^{2+} Complex. The minimized structures of both **L** and its Mg^{2+} complex were obtained through MM computations using Hyperchem software (SI11, SI12, SI13 in the Supporting Information).[8] The **L** shows a bend in each of the arms, while the resultant loop connecting the arms is unsymmetrical (Figure 7a). However, the MM minimized $[L^{2-}{\cdot}Mg^{2+}.(CH_3CO_2H)_2]$ complex shows a planar binding core wherein one of the salicylidene moieties and the phenylene present in the cap turn to form a plane utilizing the second unit of the salicylidene moiety. This results in the formation of N_2O_2 core which binds to Mg^{2+} and exhibits a different conformer of **L** when bound to the Mg^{2+}. All this is attributable to the marginal changes occurring in the dihedral angles of the bonds connecting the triazole ring and the salicylidene moiety. Since the mass spectra shows binding of two acetate moieties and from the NMR it is

dx.doi.org/10.1021/jo500892r | J. Org. Chem. 2014, 79, 5763−5770

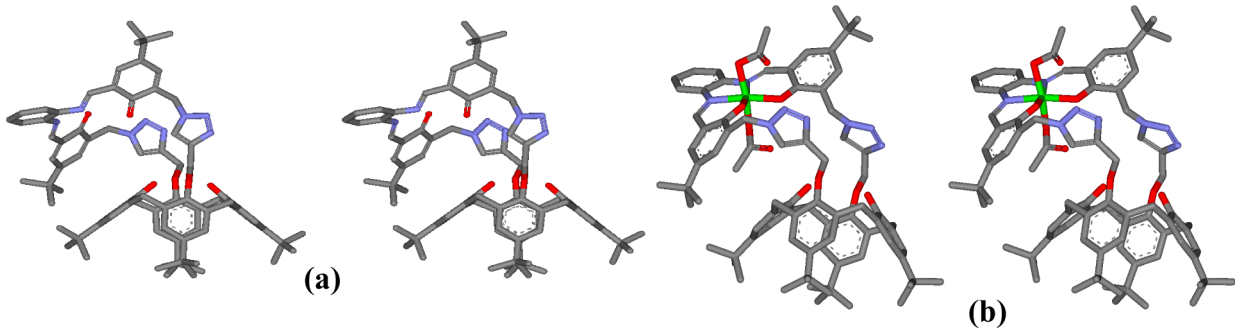

Figure 7. Stereo views of the molecular structures: MM minimized structures in case of, (a) **L** and (b) $[\mathbf{L}^{2-}\cdot Mg^{2+}\cdot(CH_3CO_2H)_2]$. Hydrogens were omitted in this figure for clarity. The calculated metric data around the magnesium sphere are given here. Bond distances: O1−Mg = 1.980; N1−Mg = 2.045; O2−Mg = 1.980; N2−Mg = 2.043; O3−Mg = 2.036; O4−Mg = 2.036. Bond angles: O1−Mg−N1 = 93.2; O1−Mg−O2 = 90.4; O1−Mg−N2 = 168.7; O1−Mg−O3 = 107.2; O1−Mg−O4 = 86.1; N1−Mg−O2 = 170.6; N1−Mg−N2 = 82.1; N1−Mg−O3 = 84.8; N1−Mg−O4 = 85.8; O2−Mg−N2 = 95.7; O2−Mg−O3 = 85.8; O2−Mg−O4 = 103.1; N2−Mg−O3 = 82.7; N2−Mg−O4 = 83.3; O3−Mg−O4 = 164.1.

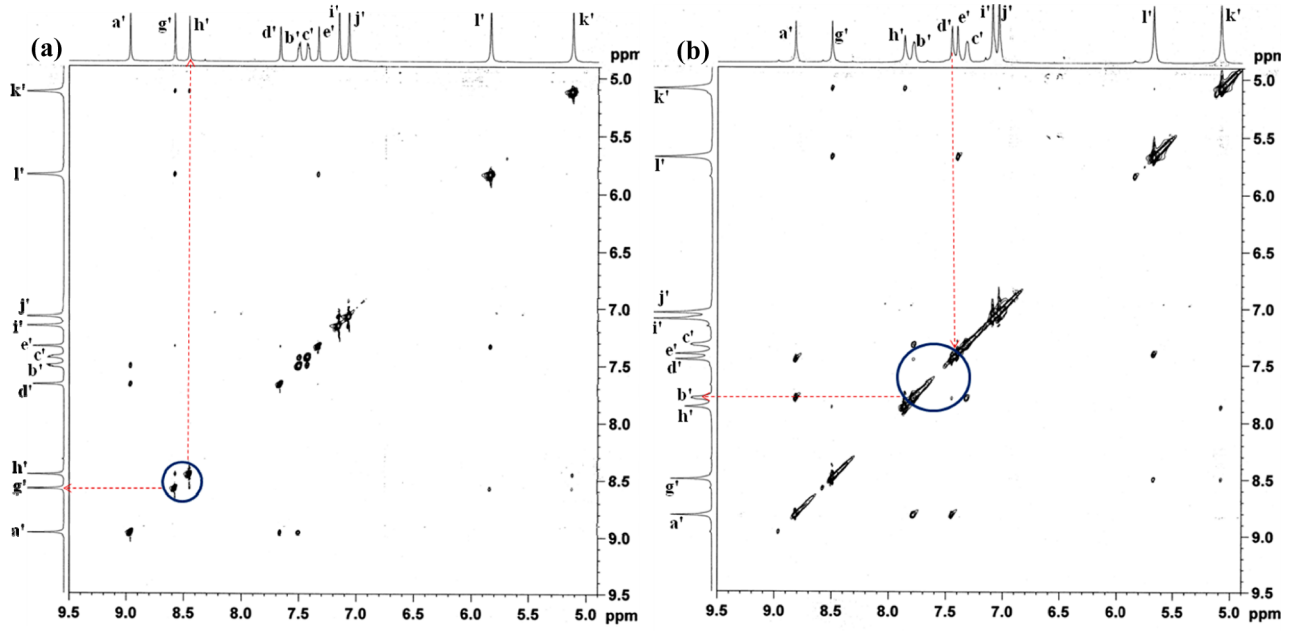

Figure 8. 2D NOESY spectrum of (a) **L** and (b) **L**+ Mg^{2+}.

understood that the acetate removes proton from phenolic−OH groups, the complex was minimized in MM+ in the presence of two equivalents of acetic acid to result in an octahedral complex for Mg^{2+} with both the acetic acid moieties being bound in *trans*-fashion exhibiting a O3−Mg−O4 angle of 164.1°. The methyl groups of both the acetic acid moieties orient toward phenyl ring that is present in the corresponding arm. Thus, the C−H of one of these methyls is oriented toward the phenyl moiety of the calix[4]arene platform. Such interaction is expected to shift the C−H chemical shift to upfield, which in fact is observed in ^{1}H NMR (SI 09 in the Supporting Information). Though this core is not in the plane in the organic receptor molecule, **L**, the same is brought into the plane but with some deviation by one of the phenolate-O^- when Mg^{2+} binds and hence acquires distortion in the geometry. Thus, the geometry of Mg^{2+} is distorted octahedrally (Figure 7b). The conformational changes occurring in the arms upon Mg^{2+} binding can be further gauged by the changes observed in the angle between the planes of both the triazole moieties (from 42.1 to 85.1°) and the arm phenyl moieties (from 52 to 39.8°). Even these changes clearly support that the arm conformation is different in its complex when compared to the simple **L**.

NOESY. The conformational change occurring in the capped arms has been supported by two-dimensional NMR, viz., NOESY (Figure 8). In the case of **L**, protons "g′" and "h′" exhibit correlation which supports the proximity of these two centers. This propinquity could also be seen from the minimized structure of **L** wherein "g′" is located inward, viz., into the calixarene cavity, and the distance between "g′" and "h′" is 2.25 Å (SI 11 in the Supporting Information). As per the computational studies carried out for the complex, the "g′" turns outward from the cavity and is no longer proximal to "h′". This result from the computation is supported by NOESY, since no correlation was noticed between "g′" and "h′". Another set of protons "b′" and "d′" shows no correlation in NOESY in the case of **L**, and this is supported by the long-range separation of 4.9 Å observed between these two proton centers in the computationally minimized structure. In the presence of Mg^{2+} the bent arm provides a near planar core as a result of the conformational changes occurring in the capped arms, and this brings "b′" and "d′" closer (4.5 Å) (SI 11 in the

dx.doi.org/10.1021/jo500892r | J. Org. Chem. 2014, 79, 5763−5770

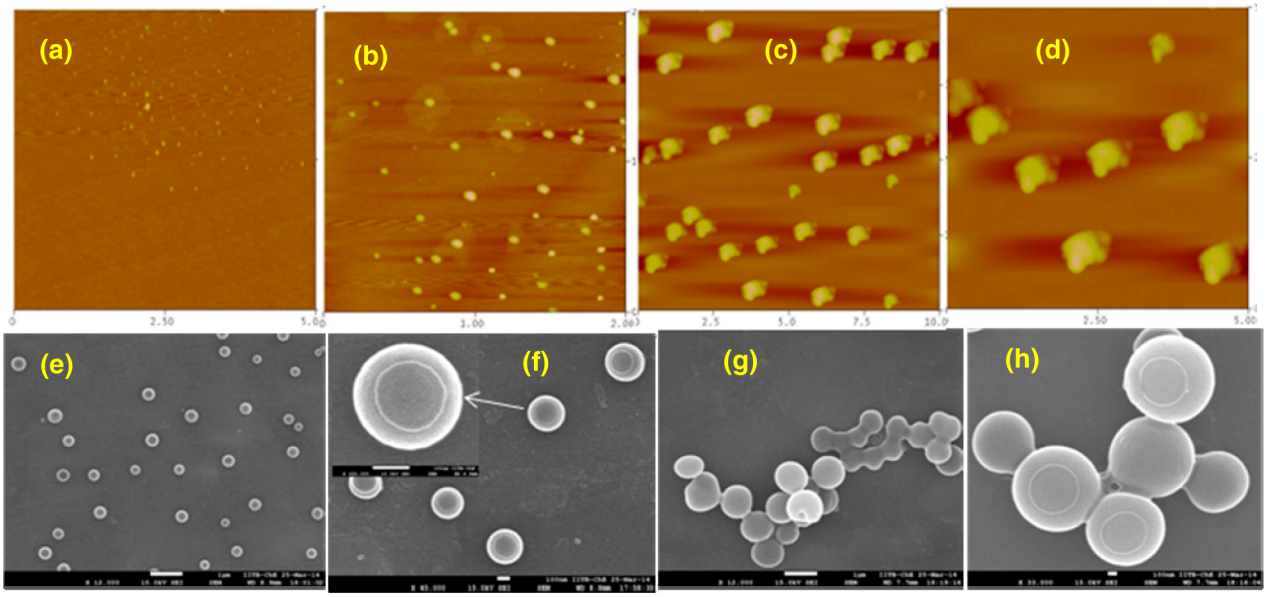

Figure 9. Microscopy images of **L** and {**L** + Mg^{2+}}. Atomic force microscopy (AFM) images are shown in the upper row: (a) **L** at 5 μm scale; (b) **L** at 2 μm scale; (c) {**L** + Mg^{2+}} at 10 μm and (d) {**L** + Mg^{2+}} at 5 μm. Scanning electron microscopy (SEM) images are shown in the bottom row: (e) **L** at 1 μm scale; (f) **L** at 1 μm with higher magnification, and the inset is one particle shown at 100 nm scale; (g) {**L** + Mg^{2+}} at 1 μm and (h) {**L** +Mg^{2+}} at 100 nm scale.

Supporting Information) and corroborates the correlation seen in the NOESY.

Microscopy Studies. Since the calix[4]arene derivatives are known to exhibit supramolecular structures, both **L** and its magnesium complex {**L** + Mg^{2+}} were studied for their nanofeatures by atomic force microscopy (AFM) (Figure 9a–d) and scanning electron microscopy (SEM) (Figure 9e–h). In the AFM, spherically shaped particles were found for **L** which are distributed on mica and exhibit a size of ∼40–50 nm where both the width and height are same. In the presence of Mg^{2+}, flower-type aggregates were seen, where the size was enlarged by several fold when compared to simple **L** wherein the height is ∼470 nm and the width is ∼980 nm. This means that about 400–800 particles of **L** are aggregated to give large flowerlike supramolecular structures in the presence of Mg^{2+} (SI 14 in the Supporting Information). Even in SEM, the spherical particles observed for **L** were linked together to form dumb-bell like structures, and these are further extended to form chainlike aggregates. Thus, both AFM and SEM support the formation of large supramolecular structures as Mg^{2+}-induced aggregation that brings the amphiphilic calix[4]conjugates together to result in aggregational fluorescence enhancement.

CONCLUSIONS AND CORRELATIONS

A triazole-linked phenylene diimine-capped conjugate of calix[4]arene, **L**, was synthesized and characterized. The receptor **L** exists in cone conformation in solution as evident from ^{1}H NMR spectra. On the basis of the fluorescence studies, it was found that **L** selectively recognizes Mg^{2+} among the biologically relevant alkali and alkali earth metal ions studied, viz.: Na^+, K^+, Mg^{2+}, and Ca^{2+}. The visual color change observed under UV light also confirms the selective recognition of Mg^{2+} by **L**. The association constant, K_a for **L** with Mg^{2+} is in the order of 10^5 M^{-1} based on fluorescence as well as absorption studies, suggesting a strong binding for Mg^{2+}. The **L** can detect Mg^{2+} up to 40 ± 5 ppb (2 μM) which is much lower than that reported in the literature.[4b,5b] Fluorescence studies supported its utility to recognize Mg^{2+} even in blood serum milieu with a minimum detection limit of 209 ± 10 ppb (8.7 μM), which is certainly lower than the Mg^{2+} present in the diluted solution of blood serum (17 μM). Even the presence of large equivalents of Na^+, K^+, or Ca^{2+} does not affect the selective recognition of Mg^{2+} by **L**. These are represented through Scheme 2.

Scheme 2. Schematic representation of "*OFF* to *ON*" behavior of L

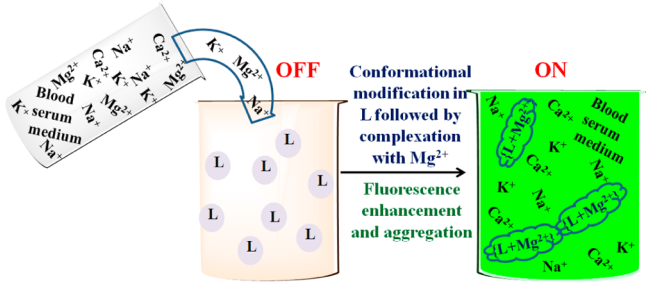

Absorption studies confirm the binding of **L** with Mg^{2+} by exhibiting an isosbestic point at 365 nm. While the Job's plot suggests the formation of a 1:1 complex between **L** and Mg^{2+}, the ESI-MS confirms the same by yielding a m/z = 1287.18 peak that is associated with the expected isotope peak pattern for magnesium. ^{1}H NMR titration data suggest the involvement of N_2O_2 core for Mg^{2+} binding as the protons present in this vicinity were affected either upfield or downfield or one followed by the other. The structure of the {**L** + Mg^{2+}} complex has been computationally addressed by molecular mechanics that found that the Mg^{2+} is bound by **L**, resulting in a distorted octahedral structure where the $\mathbf{L}^{2-}$ acts as tetradentate with an N_2O_2 core and the two acetic acid moieties binding in a *trans* manner. The conformational changes occurring in the capped arms to accommodate Mg^{2+} are indeed supported by NOESY studies. Thus, the present **L** designed by connecting the two open arms with N_2O_2 core acts

dx.doi.org/10.1021/jo500892r | J. Org. Chem. 2014, 79, 5763–5770

as a selective receptor for Mg^{2+} among the four biologically important alkali and alkaline earth ions, and the receptivity is retained even in blood serum. The differential selectivity of Mg^{2+} and Ca^{2+} toward **L** is attributable to their size difference (Ca^{2+} radius is ~30% greater than that of the Mg^{2+}) and also to their coordination preferences. While Mg^{2+} favors binding by ether oxygens, Ca^{2+} favors binding by carboxylate moieties as noticed from the biological systems. To understand the supramolecular nature of **L** and its complex with Mg^{2+}, AFM and SEM studies were carried out in which the spherically shaped particles of **L** were found enlarged as well as aggregated. Thus, the complex formation with Mg^{2+} can be differentiated from its precursor **L** by analyzing their microstructural features.

EXPERIMENTAL SECTION

General Information and Materials. The mass spectral analysis of the compounds uses the electrospray method for the ionization and quadrupole time-of-flight (Q-ToF) as mass analyzers. Distilled and deionized water was used in all the studies. Bulk solutions of **L** and the metal salts were prepared in acetonitrile at 6×10^{-4} M. All the fluorescence titrations were carried out at 339 nm excitation. Excitation and emission slit widths used were 5 nm, and the scan speed of 200 nm/min was used. All the fluorescence and absorption titrations were carried out in 1 cm quartz cells by maintaining the final [**L**] of 5 μM in a total volume of 3 mL achieved by diluting with acetonitrile.

Preparation of Blood Serum Sample. Blood serum samples were obtained from a healthy volunteer after fasting. The blood sample was allowed to clot, and serum was obtained by centrifugation. The serum samples were kept at −20 °C for storage. A 100 μL aliquot of serum was taken in 3 mL of milli Q water and used as stock solution. The fluorescence studies were performed in 10% v/v water−acetonitrile solution.

Synthesis and Characterization of 2. For the synthesis of this compound, **1** (2 g, 3.08 mmol) was dissolved in dry acetone (150 mL) to which potassium carbonate (1.03 g, 7.45 mmol) was added followed by propargyl bromide (0.950 mL, 7.45 mmol) dropwise to the reaction mixture with stirring and allowed to reflux for 24 h. The reaction mixture was filtered, and the solvent was evaporated under reduced pressure. The residue was dissolved in dichloromethane and washed with 2 N HCl (50 mL) solution and extracted with dichloromethane (3 × 50 mL). The combined organic layer was washed with distilled water (2 × 40 mL) followed by brine solution, dried over Na_2SO_4, and evaporated under reduced pressure, and then CH_3OH was added to this and triturated to afford pure white residue which was then filtered and dried under vacuum. (Yield, 1.87 g, 82%).**^{1}H NMR ($CDCl_3$, δ ppm):** 7.07 (s, 4H, Ar-**H**), 6.73 (s, 4H, Ar-**H**), 6.50 (s, 2H, O**H**), 4.74 (d, J = 2.4 Hz, 4H, OC**H**$_2$), 4.37 (d, J = 13.4 Hz, 4H, Ar-C**H**$_2$Ar), 3.33 (d, J = 13.4 Hz, 4H, Ar-C**H**$_2$Ar), 2.54 (t, J = 2.4 Hz, 2H, C**H**), 1.30 (s, 18H, (C**H**$_3$)$_3$), 0.90 (s, 18H, (C**H**$_3$)$_3$); **HRMS** m/z Calcd for $C_{50}H_{61}O_4$: 725.4570, Found 725.4576.

Synthesis and Characterization of 3. This compound was synthesized by the method reported in literature.[7a] A solution of *p-tert*-butylphenol (12.0 g, 40 mmol) in toluene (40 mL) and $SnCl_4$ (2.14 g, 48.1 mmol) in dichloromethane were taken. After completely dissolving this mixture, Bu_3N (7.834 mL, 32.8 mmol) was added dropwise via syringe, and the resultant mixture was allowed to stir for 20 min, and then $(CH_2O)_n$ (4.86 g, 162 mmol) was added to the mixture and refluxed for 8 h. After the reaction mixture cooled, it was poured into a separating funnel and extracted with diethyl ether (3 × 40 mL). The organic layer was washed with brine and dried over Na_2SO_4. The solvent was evaporated under reduced pressure, and the product was purified (4.5 g) by column chromatography using ethyl acetate/petroleum ether (1:9) as eluants. Yield (63%). **^{1}H NMR ($CDCl_3$, δ ppm)** 1.25 (s, 9H, C-(C**H**$_3$)$_3$), 6.86 (s, 1H, Ar-**H**, J = 9.1 Hz), 7.44 (d, 1H, Ar-**H**, J = 2.4 Hz), 7.52 (dd, 1H, Ar-**H**, J = 2.4 Hz), 9.82 (s, 1H, Ar-C**H**O), 10.80 (s, 1H, Ar-O**H**). **HRMS** m/z Calcd for $C_{11}H_{15}O_2$: 179.1072, Found 179.1072.

Synthesis and Characterization of 4. A mixture of 5-(*tert*-butyl)-2-hydroxybenzaldehyde (1.0 g, 5.68 mmol), formaldehyde (30 mL), and 100 mL HCl (33%) were taken, and this solution was stirred for 48 h at room temperature. After the aldehyde was consumed, water was added to the reaction mixture in an excess amount, and the mixture stirred for 15 min and then was extracted with CH_2Cl_2 (3 × 30 mL). The combined organic layer was washed with water (3 × 40 mL) followed by brine and dried over Na_2SO_4. Evaporation of the solvent under reduced pressure resulted in a pure yellow-colored compound as liquid (1.2 g). Yield (82%). **^{1}H NMR ($CDCl_3$, δ ppm):** 1.34 (s, 9H, C-(C**H**$_3$)$_3$), 4.70 (s, 2H, C**H**$_2$Cl), 7.52 (d, 1H, Ar-**H**, J = 2.4 Hz), 7.67 (d, 2H, Ar-**H**, J = 2.5 Hz), 9.90 (s, 1H, Ar-O**H**), 11.28 (s, 1H, Ar-C**H**O). m/z **(ES/MS)** 191.18 ([M − Cl + H]$^+$).

Synthesis and Characterization of 5. To a solution of 5-*tert*-butyl-3-(chloromethyl)-2-hydroxybenzaldehyde (1.00 g 4.41 mmol) in 15 mL dimethylformamide, was added NaN_3 (0.574 g, 8.823 mmol) and stirred for 12 h at room temperature. After completing the reaction, water was added in excess, and then the reaction mixture was extracted with ethyl acetate (5 × 20 mL) which was further washed with brine solution and dried over Na_2SO_4. The solvent was evaporated under reduced pressure to afford the compound (0.850 g) as liquid. (Yield 89%). **^{1}H NMR ($CDCl_3$, δ ppm):** 11.2 (broad s, H, Ar-O**H**), 9.99 (s, H, C**H**O), 7.55 (dd, 1H, Ar-**H**), 7.59 (s, 1H, Ar-**H**), 4.48 (s, 2H, Ar-C**H**$_2$), 1.35 (s, 9 H, Ar-(C**H**$_3$)$_3$). **IR** ν_{max} = 2964, 2869, 2104, 1655. m/z **(ES/MS)** 191.18 ([M − N_3 + H]$^+$).

Synthesis and Characterization of L′. To synthesize this compound, **2** (1.00 g, 1.38 mmol) and **5** were dissolved in 20 mL of a mixture of dichloromethane, *tert*-butanol, and water in 1:1:2 volume ratio. To this solution, were added $CuSO_4 \cdot 5H_2O$ (0.04 g, 0.015 mmol) and sodium ascorbate (0.063 mg, 0.3 mmol) which caused change in the color of reaction mixture which was then stirred for 12 h at room temperature. After completion of the reaction, 20 mL of water was added to the reaction mixture which was then extracted with dichloromethane (3 × 20 mL). The combined dichloromethane layers were washed with water (30 mL), followed by brine solution, and then were dried over Na_2SO_4. The solvent was evaporated under reduced pressure to afford a liquid compound which was purified by triturating in hexane (50 mL) to afford a white-colored precipitate that was filtered and then dried under vacuum (1.2 g). Yield 90%. **^{1}H NMR ($CDCl_3$, δ ppm):** 11.30 (s, 2H, Sal-O**H**), 9.83 (s, 2H, sal-C**H**O), 8.08 (s, 2H, triazole-**H**), 7.62 (s, 2H, Sal-**H**) 7.49 (d, 2H, Sal-**H**), 7.15 (s, 2H, Ar-O**H**), 6.98 (s, 4H, Ar-**H**), 6.77 (s, 4H, Ar-**H**), 5.56 (s, 2H, Sal-C**H**$_2$), 5.18 (s, 2H, Ar-O-C**H**$_2$), 4.14 (d, J = 13.0 Hz, 4H, Ar-C**H**$_2$-Ar), 3.17 (d, J = 13.0 Hz, 4H, Ar-C**H**$_2$-Ar), 1.27 (s, 18H, Ar-(C**H**$_3$)$_3$), 1.26 (s, 18H, Ar-(C**H**$_3$)$_3$), 0.96 (Sal-(C**H**$_3$)$_3$).**^{13}C NMR ($CDCl_3$, δ ppm):** 196.7, 157.3, 150.5, 149.8, 147.3, 144.5, 143.3, 141.6, 135.4, 134.28, 134.27 132.7, 130.8, 127.9, 125.8, 125.2, 124.2, 123.2, 120.3, 70.0, 48.3, 34.3, 34.1 33.9,

dx.doi.org/10.1021/jo500892r | J. Org. Chem. 2014, 79, 5763−5770

31.8, 31.3, 31.1. *m/z* (ES/MS) 1129.08 (([M + H]$^+$), 1146.20 ([M + Na]$^+$).

Synthesis and Characterization of L. The compound L′ (1.00 g, 0.839 mmol) was dissolved in 20 mL of methanol by heating and to this phenylenediamine (0.90 g, 0.839 mmol) was added. Immediately after the addition, the colorless solution changed to pinkish-brown. The reaction mixture was stirred for 12 h at room temperature, upon which a brown precipitate was formed; this was then filtered, washed with methanol 4−5 times, and dried under vacuum to obtain a pure product (0.8 g). Yield (74%). Mp 220−225 °C. **^{1}H NMR (DMSO-d_6, δ ppm):** 13.7 (broad s, 2H, Sal-OH), 8.7(s, 2H, Sal-imine-H), 8.3(s, 2H, triazole-H), 7.29−7.40 (m Ar-H), 7.10 (s, 2H, Ar-OH),, 6.9 (s, 4H, Ar-H), 6.8 (s, 4H, Ar-H,, 5.8 (s, 4H, Sal-CH_2), 5.1 (s, 4H, Ar-OCHH_2), 4.16(d, 4H, Ar-CH_2-Ar), 3.33(d, 4H, Ar-CH_2-Ar), 1.28 (s,18 H, -C$(CH_3)_3$), 1.24 (Ar-C$(CH_3)_3$), 0.98(s, 18 H, Ar-$(CH_3)_3$); ^{13}C NMR ($CDCl_3$, (δ ppm): 165.1, 157.2, 150.35, 150.3, 147.65, 143.3, 142.3, 141.8, 141.3, 133.9, 130.54, 130.5, 129.8, 128.5, 128.0, 126.2, 125.6, 125.2, 123.6, 119.6, 118.6, 79.5, 48.9, 34.4, 34.2, 34.0, 32.1, 31.8, 31.5, 31.4. HRMS: for $C_{80}H_{95}O_6N_8$ $[M+1]^+$ calculated: 1263.7375 found: 1263.7389.

Computational Methodology. The structures of the receptor **L** and its {**L**·Mg^{2+}} were minimized using molecular mechanics by employing the Hyperchem.[8] The initial model of **L** was generated using gauss view and was given as input for MM calculations. In order to make the neutral complex with Mg^{2+}, the salicyl-OH groups of **L** were deprotonated to give $\mathbf{L}^{2-}$ and this was used for the complexation and the corresponding input was subjected to minimization. The complex of $\mathbf{L}^{2-}$ with Mg^{2+} was made by simply placing the Mg^{2+} in the vicinity of the binding arms of the minimized $\mathbf{L}^{2-}$ in such a way that the salicyl O-, imine N- atoms point toward Mg^{2+} and were minimized. To the resultant {$\mathbf{L}^{2-}$·Mg^{2+}} complex, two acetic acid molecules were added to complete the octahedral coordination, and the resulting structure was minimized. All these minimizations were carried out with MM+ force field with steepest descent method, and the RMS gradient (0.01 kcal/(Å mol)) was used.

Sample Preparation for Microscopy Studies. Forty μL aliquots of **L** and {**L** + Mg^{2+}} in acetonitrile (5 μM) were drop casted on a freshly cleaved mica surface for AFM studies and on an aluminum surface for SEM studies and dried under an IR lamp.

■ ASSOCIATED CONTENT

Supporting Information

Characterization of precursors and spectral data. Fluorescence and absorption spectral traces. Cartesian coordinates for MM minimized **L** and its Mg^{2+} complex. Microscopy image. This material is available free of charge via the Internet at http://pubs.acs.org.

■ AUTHOR INFORMATION

Corresponding Author

*Telephone: 91 22 2576 7162. Fax: 91 22 2572 3480. E-mail:cprao@iitb.ac.in.

Notes

The authors declare no competing financial interest.

■ ACKNOWLEDGMENTS

C.P.R. acknowledges the financial support from DST, CSIR, and DAE-BRNS. A.N. acknowledges the UGC for a fellowship. We thank Mr. Tippa D. Venkata Satyanarayana for some experimental help. We acknowledge the FEG-SEM and SPM facilities of IIT Bombay for extending their services.

■ REFERENCES

(1) (a) Stepura, O. B.; Martynow, A. I. *Int. J. Cardiol.* **2009**, *134*, 145−147. (b) Larsson, S. C.; Virtanen, M. J.; Mars, M.; Männisto, S.; Pietinen, P.; Albanes, D.; Virtamo, J. *Arch. Int. Med.* **2008**, *168*, 459−465. (c) Rubin, H. *Arch. Biochem. Biophys.* **2007**, *458*, 16−23. (d) Cowan, J. A. *BioMetals* **2002**, *15*, 225−235.

(2) Saris, N. E. L.; Mervaala, E.; Karppanen, H.; Khawaja, J. A.; Lewenstam, A. *Clin. Chim. Acta* **2000**, *294*, 1−26.

(3) (a) Dong, Y.; Mao, X.; Jiang, X.; Hou, J.; Cheng, Y.; Zhu, C. *Chem. Commun.* **2011**, *47*, 9450−9452. (b) Dong, Y.; Li, J.; Jiang, X.; Song, F.; Cheng, Y.; Zhu. *Org. Lett.* **2011**, *13*, 2252−2255.

(4) (a) Singh, N.; Kaur, N.; Mulrooney, R. C.; Callan, J. F. *Tetrahedron Lett.* **2008**, *49*, 6690−6692. (b) Saluja, P.; Sharma, H.; Kaur, N.; Singh, N.; Jang, D. O. *Tetrahedron* **2012**, *68*, 2289−2293. (c) Kim, J.; Morozumi, T.; Nakamura, H. *Org. Lett.* **2007**, *9*, 4419−4422. (d) Liu, Y.; Han, M.; Zhang, H. Y.; Yang, L. X.; Jiang, W. *Org. Lett.* **2008**, *10*, 2873−2876. (e) Hama, H.; Morozumib, T.; Nakamura, H. *Tetrahedron Lett.* **2007**, *48*, 1859−1861.

(5) (a) Hamdi, A.; Kim, S. H.; Abidi, R.; Thuery, P.; Kim, J. S.; Vicens, J. *Tetrahedron* **2009**, *65*, 2818−2823. (b) Song, K. C.; Choi, M. G.; Ryu, D. H.; Kim, K. N.; Chang, S. K. *Tetrahedron Lett.* **2007**, *48*, 5397−5400.

(6) (a) Gutsche, C. D.; Dhawan, B.; No, K. H.; Muthukrishnan, R. *J. Am. Chem. Soc.* **1981**, *103*, 3782−3792. (b) Janssen, R. G.; Verboom, W.; Reinhoudt, D. N.; Casnati, A.; Freriks, M.; Pochini, A.; Ugozzoli, F.; Ungaro, R.; Nieto, P. M.; Carramolino, M.; Cuevas, F.; Prados, P.; Mendoza, J. D. *Synthesis* **1993**, 380−386. (c) Duynhoven, J. P. M. V.; Janssen, R. G.; Verboom, W.; Franken, S. M.; Casnati, A.; Pochini, A.; Ungaro, R.; Mendoza, J. D.; Nieto, P. M.; Pradas, P.; Reinhoudt, D. N. *J. Am. Chem. Soc.* **1994**, *116*, 5814−5822.

(7) (a) Joseph, R.; Rao, C. P. *Chem. Rev.* **2011**, *111*, 4658−4702. (b) Pathak, R. K.; Dikundwar, A. G.; Guru Row, T. N.; Rao, C. P. *Chem. Commun.* **2010**, *46*, 4345−4347. (c) Bandela, A.; Chinta, J. P.; Rao, C. P. *Dalton Trans.* **2011**, *40*, 11367−11370. (d) Pathak, R. K.; Hinge, V. K.; Mondal, M.; Rao, C. P. *J. Org. Chem.* **2011**, *76*, 10039−10049. (e) Zhao, J.; Zhao, B.; Liu, J.; Ren, A.; Feng, J. *Chem. Lett.* **2006**, 268−274. (f) Wang, L.; Qin, W.; Tang, X.; Dou, W.; Liu, W. *J. Phys. Chem. A* **2011**, *115*, 1609−1616. (g) Gorner, H.; Khanra, S.; Weyhermuller, T.; Chaudhari, P. *J. Phys. Chem. A* **2006**, *110*, 2587−2594. (h) Wang, L.; Qin, W.; Liu, W. *Inorg. Chem. Commun.* **2010**, *13*, 1122−1126. (i) Wu, J.; Ge, J.; Zhang, H.; Wang, P. *Chem. Soc. Rev.* **2011**, *40*, 3483−3495.

(8) *Hyperchem 8.0.4*; Hypercube, Inc.: Gainesville, FL, 2007.